ELSEVIER

Catalysis Today 32 (1996) 149–156

CATALYSIS TODAY

Methane partial oxidation to synthesis gas using nickel on calcium aluminate catalysts

M.A. Goula [a,*], A.A. Lemonidou [a], W. Grünert [b], M. Baerns [b]

[a] *Chemical Process Engineering Research Institute and Department of Chemical Engineering, Aristotle University of Thessaloniki, P.O. Box 361, 570 01 Thermi, Thessaloniki, Greece*

[b] *Ruhr-Universität Bochum, Lehrstuhl für Technische Chemie, P.O. Box 102 148, D-44 780 Bochum, Germany*

Abstract

Nickel was supported on calcium aluminate carriers that were obtained with varying CaO to Al_2O_3 molar ratios and calcination temperatures. The variations of the supports lead to catalysts of different surface properties and catalytic performance. Metallic nickel (Ni^0) was proven to be the active species for the methane partial oxidation reaction. The presence of filamentous carbon on used catalysts was also suggested. The differences in the catalytic activity and selectivity for the methane partial oxidation reaction was ascribed to a varying degree of reducibility of the surface nickel species.

Keywords: Synthesis gas; Nickel catalysts; Methane partial oxidation

1. Introduction

Synthesis gas is produced from methane mainly by steam reforming which suffers from limitations, like high energy requirements and high H_2/CO ratio. It is also produced by non catalytic partial oxidation reaction which is mildly exothermic, but operates at very severe conditions. Recently, much effort has been devoted to partial oxidation of methane to syngas in the presence of catalysts. Noble and transition supported metals were found to be very active and selective at low temperatures.

Nickel catalysts supported on alumina [1–6] have been extensively used for the conversion of methane to syngas. On the other hand, calcium aluminate mixed oxides were found to be very stable and active catalysts in hydrocarbon cracking as well as in the reforming of heavy hydrocarbons with very low coke deposition [7,8]. The aim of the present work was to elucidate the changes on the catalytic surface during the methane partial oxidation reaction and clarify the determining factor for catalytic activity and selectivity. For this reason, bulk and surface characterisation techniques were applied to fresh and used catalysts, in an effort to find the correlation between the characteristic properties and their catalytic performance.

2. Experimental

2.1. Catalyst preparation

The carriers employed for the preparation of supported nickel catalysts were mechanical mix-

---

[*] Corresponding author.

PII S0920-5861(96)00168-X

tures of $CaCO_3$ (Mallinckrot, Analytical Reagent) and γ-Al_2O_3 (Catapal alumina) calcined at 1100 or 1300°C. Mixtures consisting of CaO/Al_2O_3 molar ratio of 1:2 (support A) and 12:7 (support B) were used in the present work. Details on the preparation and calcination procedures of the carriers employed can be found elsewhere [9]. Catalysts were prepared by the method of incipient wetness impregnation using an aqueous solution of nickel nitrate, so as to yield 5 or 1 wt% metal loading. The resulting materials were then dried and calcined in air for 4 h at 600°C and for 10 h at 900°C.

NiO was used as supplied as standard material for the XPS experiments. The $NiAl_2O_4$ standard was prepared from a solution of $Ni(NO_3)_2 \cdot 6H_2O$ and $Al(NO_3)_3 \cdot 9H_2O$ by drying and calcination for 2 h in air at 900°C.

2.2. Characterisation

The specific surface area of catalysts and supports was determined using the BET technique with a Micromeritics Accusorb 2100E. Pure nitrogen (Linde special) and helium (Linde 99.996%) were used as adsorbate and inert gas, respectively.

Crystal phases were identified by X-ray diffraction analysis using a Siemens D500 diffractometer equipped with a Kristalloflex 710H X-ray generator, an X-ray anode tube of Cu and a Ni K_b filter.

Fresh and used catalysts have been characterized for their surface properties using X-ray photoelectron spectroscopy (the total reactor loading was analysed after the reaction). XPS spectra were recorded using a Leybold LHS 10 spectrometer, equipped with a Single Channel Detector with AlK alpha radiation (power settings: 12 kV * 23 mA). The analyser was used in the pass energy mode, with a pass energy of 100 eV. Powdered samples were pressed and mounted on a standard sample probe, evacuated in a pre-evacuation chamber down to ca. 10^{-5} Torr (1 Torr = 133.3 Pa), before they were moved into the main vacuum chamber. The residual pressure in the turbo-pumped analysis chamber was kept below 5×10^{-8} Torr during data collection. Each spectral region was signal-averaged for a given number of scans to obtain good signal-to-noise ratios. Although surface charging was observed on all the samples, accurate binding energies were determined by charge referencing with the Ca2p line 347.0 eV. With this calibration, binding energies of 284.5 to 285.1 eV were obtained for adventitious carbon. Peak fitting for the Ni 2p signal was performed with a programme using Voigt-type lines (80% Gaussian contribution), after removal of a Shirley-type background. Atomic ratios were calculated from intensity ratios using Scofield sensitivity factors [10] together with an experimentally derived response function of our spectrometer to the variation of the photoelectron kinetic energy. Peak areas of Ni^{2+} were computed by a program which assumed Gaussian lines and a Shirley-type background.

The total carbon content on catalysts after the reaction time were measured by an CHN-800 (LECO Corp.) elemental analyser, having a carbon sensitivity 0.01%.

2.3. Catalyst testing

Catalysts were tested in a conventional flow apparatus using a quartz reactor at atmospheric pressure. The reaction temperature was 750°C with a CH_4/O_2 ratio equal to 2/1 and a total space time of 6 $kg \cdot s \cdot mol^{-1}$. Helium (He) was used as a diluent (50 volume%). The reaction products were analyzed using a Varian 37 gas chromatograph equipped with a TC detector. Two columns Porapak Q and MS 5A were used in a series/ by pass arrangement for the complete separation of H_2, O_2, CH_4, CO and CO_2. The catalysts were prereduced in H_2 flow at 750°C for 1 h before testing. The reaction time was 2 h. Furthermore, for the catalyst 5 wt% Ni on support A longer reaction times (20 h) were used for stability measurements.

3. Results

The XPS binding energies (Ni^{2+} $2p_{3/2}$, Fig. 1) of the catalysts are between those of NiO and $NiAl_2O_4$, with line widths exceeding those found with the pure reference compounds. This indicates a coexistence of the oxide and aluminate like species in the surface region. This conclusion was confirmed by XRD for catalysts supported on support A (Table 1). On the other side, for catalysts supported on support B neither $NiAl_2O_4$ nor α-Al_2O_3 has been observed at their XRD spectra. So, their high values of the Ni^{2+} $2p^{3/2}$ binding energy may not necessarily be attributed to the presence of nickel aluminate spinel phase at their surface.

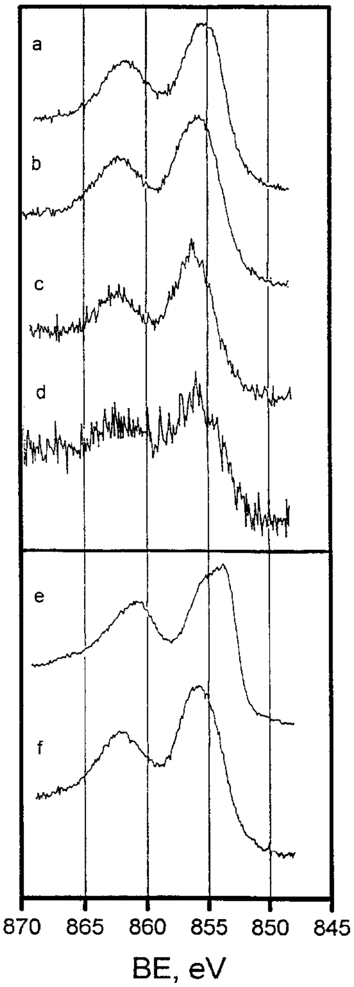

Fig. 1. XPS spectra of Ni^{2+} $2p^{3/2}$ level for fresh catalysts and standards (a: support A–5% Ni, b: support B–5% Ni, c: support A–1% Ni, d: support B–1% Ni, e: NiO and f: $NiAl_2O_4$).

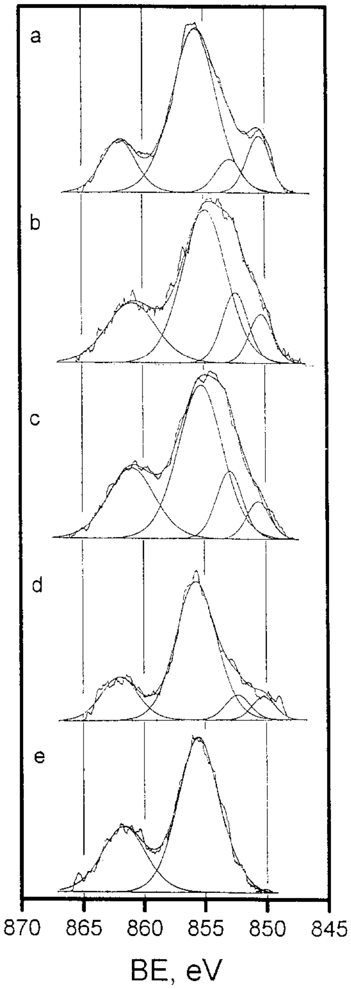

Fig. 2. XPS spectra of Ni^{2+} $2p^{3/2}$ level for used catalysts (a: support A–5% Ni {stability}, b: support A–5% Ni, c: support B–5% Ni, d: support A–1% Ni, e: support B–1% Ni).

The nickel spectra, on the other hand, were very different after the reaction for all of the catalysts (Fig. 2). A new peak, at about 852.6 eV, was observed which was assigned to metallic Ni [11–13]. The only sample, for which *no* metallic nickel has been detected on its surface, was the one with 1 wt% Ni content and supported on support B. Another signal appeared at 850 eV in all used catalysts except for the previous one. After comparing curves (a) and

Table 1
Crystal phases of the catalysts determined by XRD analysis

Samples	Ni^{2+} crystal phases	Support crystal phases
Support A	–	$CaAl_4O_7$, $CaAl_2O_4$, α-Al_2O_3
Support A–1 wt% Ni (fresh)	NiO, $NiAl_2O_4$	$CaAl_4O_7$, $CaAl_2O_4$, α-Al_2O_3
Support A–1 wt% Ni (used)	NiO, $NiAl_2O_4$, Ni	$CaAl_4O_7$, $CaAl_2O_4$, α-Al_2O_3
Support A–5 wt% Ni (fresh)	NiO, $NiAl_2O_4$	$CaAl_4O_7$, $CaAl_2O_4$, α-Al_2O_3
Support A–5 wt% Ni (used)	NiO, $NiAl_2O_4$, Ni	$CaAl_4O_7$, $CaAl_2O_4$, α-Al_2O_3
Support A–5 wt% Ni (stab.)	NiO, $NiAl_2O_4$, Ni	$CaAl_4O_7$, $CaAl_2O_4$, α-Al_2O_3
Support B	–	$Ca_{12}Al_{14}O_{33}$, $Ca_3Al_2O_6$
Support B–1 wt% Ni (fresh)	NiO	$Ca_{12}Al_{14}O_{33}$, $Ca_3Al_2O_6$
Support B–1 wt% Ni (used)	NiO	$Ca_{12}Al_{14}O_{33}$, $Ca_3Al_2O_6$
Support B–5 wt% Ni (fresh)	NiO	$Ca_{12}Al_{14}O_{33}$, $Ca_3Al_2O_6$
Support B–5 wt% Ni (used)	NiO, Ni	$Ca_{12}Al_{14}O_{33}$, $Ca_3Al_2O_6$

(b), it might be said that metallic nickel was formed during the reduction stage (the areas under the 852.8 and 850.5 eV peaks indicate this).

Concerning carbon peaks, three types of carbon were identified for all of the samples (Fig. 3, Fig. 4). These were carbonates (288.5–289.8 eV), elemental carbon (284.5–285.1 eV) and a peak with a binding energy of 282.5–283.4 eV. Their contribution to the total carbon signal was very different. Generally, the elemental carbon or the low-BE peak was the predominant one for catalysts supported on B or A calcium aluminate phase, respectively. Furthermore, an increase of the low-BE peak was observed for the catalysts after the partial oxidation reaction (except for the 1 wt% Ni on support A).

From Table 2 it is shown that the activity and

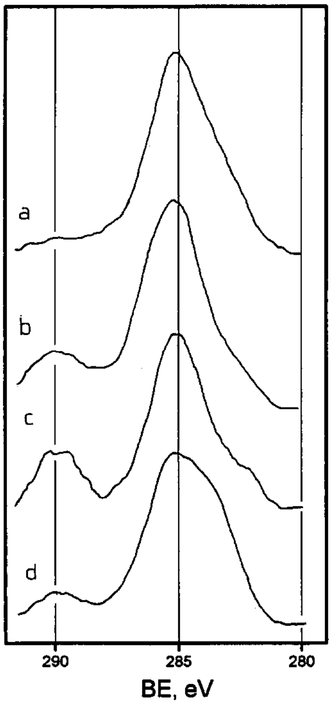

Fig. 3. XPS spectra of C1s level for catalysts supported on support A (a: 5% Ni {stability}, b: 5% Ni {used}, c: 5% Ni {fresh}, d: 1% Ni {used}, e: 1% Ni {fresh}).

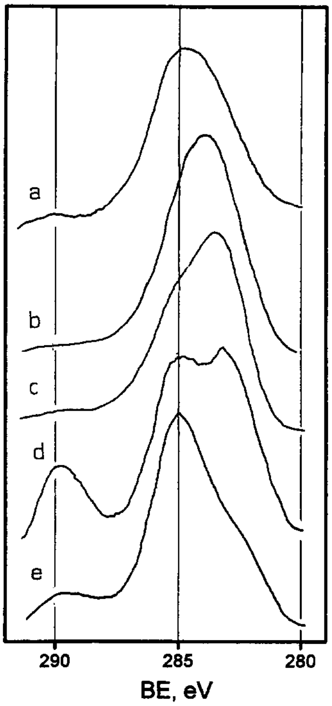

Fig. 4. XPS spectra of C1s level for catalysts supported on support B (a: 5% Ni {used}, b: 5% Ni {fresh}, c: 1% Ni {used}, d: 1% Ni {fresh}).

Table 2
Catalytic testing results

Catalysts	Conversion (%)		Selectivity		Coke (wt%)
	CH_4	O_2	CO	CO_2	on catalyst
Support A–5 wt% Ni (stability)	85.0	100	89.9	10.1	1.25
Support A–5 wt% Ni	85.0	100	89.9	10.1	1.54
Support A–1 wt% Ni	69.0	100	75.0	25.0	0.45
Support B–5 wt% Ni	84.0	100	89.5	10.5	2.52
Support B–1 wt% Ni	25.9	93.2	17.5	82.5 [a]	0.25

[a] Traces of C_2 hydrocarbons were observed.

the CO selectivity of the samples with 5 wt% nickel content is very high and about the same for the two catalysts, irrespective of the type of support. After decreasing the metal loading from 5 to 1 wt% for support A relatively lower activity was observed. The decrease in activity was more pronounced for the 1 wt% nickel catalyst on support B where the CH_4 conversion and CO selectivity was 26% and 17.5, respectively. For the catalyst 5 wt% Ni on support A, which was tested for extended period of time, it was found that the activity remained constant after 20 h of operation at 750°C, even though coke deposition was observed on its surface after the reaction. The oxygen conversion was almost 100% for all of the catalysts, whereas the CO_2 selectivity was relatively low for the very active catalysts and rather high for the inactive one.

From the catalytic testing results it was suggested that catalysts with 5 wt% Ni content revealed the same activity and selectivity, while for low nickel content catalysts these values were very different. The Ni dispersion in the near surface layer was assessed for the fresh catalysts by combining the Ni/(Al + Ca) atomic ratio with the BET data reported in Table 3. This assessment is based on the consideration, that for samples with identical Ni content, the Ni/(Al + Ca) ratio should increase at rather the same rate as the BET surface area decreases, provided that all Ni remains in the sampling depth of XPS. From the catalyst classification according to their Ni surface concentration Sup. A–1 wt% Ni = Sup. A–5 wt% Ni > Sup. B–5 wt% Ni = Sup. B–1 wt% Ni was suggested that there is no correlation between dispersion and catalytic performance.

Furthermore, in Table 3 it is shown that support B, as well as, catalysts supported on it have very low BET values, while support A and catalysts supported on its surface have medium values of SSA. For both catalytic systems an increase in the specific surface area was observed after deposition of 1 wt% Ni and a subsequent decrease for 5 wt% Ni. This was attributed to the fact that for the low nickel content catalysts the presence of the $NiAl_2O_4$ or the Ni–calcium aluminate mixed phase may give rise to additional BET area, while for those of high nickel content a multilayer of nickel oxide phase has been developed at the surface

Table 3
Specific surface area of fresh catalysts and supports

Samples	CaO/Al_2O_3 molar ratio	Tcalc.sup. (°C)	Tcalc.cat. (°C)	SSA ($m^2\ gr^{-1}$)
Support A	1/2	1100	900	8.7
Support A–1 wt% Ni	1/2	1100	900	11.5
Support A–5 wt% Ni	1/2	1100	900	6.6
Support B	12/7	1300	900	0.3
Support B–1 wt% Ni	12/7	1300	900	2.7
Support B–5 wt% Ni	12/7	1300	900	1.6

Table 4
Atomic intensity ratios from XPS analysis

Catalysts	$n_{Ni}/(n_{Al}+n_{Ca})$	n_{Ni}/n_C
Support A–5 wt% Ni (fresh)	0.162	0.151
Support A–5 wt% Ni (used)	0.095	0.063
Support A–5 wt% Ni (stab.)	0.041	0.049
Support A–1 wt% Ni (fresh)	0.021	0.033
Support A–1 wt% Ni (used)	0.018	0.015
Support B–5 wt% Ni (fresh)	0.244	0.276
Support B–5 wt% Ni (used)	0.179	0.036
Support B–1 wt% Ni (fresh)	0.021	0.022
Support B–1 wt% Ni (used)	0.024	0.064

causing the lowering at the SSA values. It seems that the interaction between Ni and Al_2O_3 or the Ca–Al–O phases leads to a roughening of the surface, which is demonstrated by the BET results.

In Table 4, the Ni/(Al + Ca) and Ni/C atomic ratios are presented. It was observed that for used catalysts the nickel to aluminum plus calcium ratio decreases in all cases (except of the 1 wt% Ni samples). The reason for this decrease might be either agglomeration of the nickel species during the reaction or preferential carbon deposition on nickel metal particles. It could be speculated that the first case is rather valid for catalysts supported on support B and the second for catalysts supported on support A.

The nickel to carbon ratio, on the other hand, decreases drastically for the high nickel content ''used'' catalysts, suggesting carbon deposition during the reaction [14,15]. More carbon seems to be deposited on the surface of the catalyst with the higher molar ratio CaO/Al_2O_3 in the bulk phase. For the low nickel content catalysts, on the other side, no appreciable carbon deposition has been detected. These findings are also supported from the coke on catalyst measurements after the reaction (Table 2).

4. Discussion

The calcium aluminates, that have been used as supports in this study, should be considered as two extreme cases concerning their attitude towards nickel deposition on their surface. The first one, consisting of $CaAl_4O_7$ and $CaAl_2O_4$ crystal phases, had a medium surface area and has been characterized as an ''open'' support. The second one, consisting mainly of $Ca_{12}Al_{14}O_{33}$ mixed oxide, had a very low surface area and has been characterized as a ''dense'' support.

Nickel catalysts supported on an ''open'' calcium aluminate A revealed variations in the value of their $Ni2p^{3/2}$ binding energy (eV) with lowering their total nickel content from 5 to 1 wt%. This reflects differences in the nature of the surface nickel species. Specifically, presence of spinel $NiAl_2O_4$ was suggested for the low nickel content catalyst. NiO was mainly present at the high nickel content catalyst, as after nickel saturates the surface sites of alumina not engaged in Ca–Al phases, further addition of nickel could be accommodated only by formation of a separate phase on top of the spinel layer. This was also supported by XRD results (Table 1).

The opposite is valid for the other case, catalysts supported on a ''dense'' calcium aluminate, where no differences were observed for the $Ni2p^{3/2}$ binding energies. Moreover, no $NiAl_2O_4$ has been detected on these catalysts and no ''residual'' Al_2O_3 has been observed on the calcined support by XRD analysis. So, one could ascribe the high E_b values to strong interaction between the Ca–Al–O phase and the Ni ions. This interaction has not lead, however, to an increased dispersion, which may be due to an incorporation of Ni species into the bulk of the $Ca_{12}Al_{14}O_{33}$ crystal phase.

XPS experiments on used catalysts revealed a new peak at about 852.6 eV and it was assigned to metallic nickel. The only sample for which no Ni^0 was detected on its surface was the one with 1 wt% nickel content and supported on support B. Furthermore, a decrease on the nickel dispersion and an appreciable carbon deposition during the partial oxidation reaction was observed for the high nickel content catalysts. These samples exhibited almost the same catalytic performance, irrespective of the support.

On the contrary, catalysts containing 1 wt% Ni on their bulk phase were very different concerning their activity and selectivity. Specifically, the one supported on support A was more active than the other supported on support B (CH_4 conversion 69% and 26%, respectively). This difference could be attributed to the absence of the metallic nickel peak from the spectra of the second catalyst, suggesting that the low activity is due to the low reducibility of Ni^{2+} interacting with the $Ca_{12}Al_{14}O_{33}$ phase [16] or incorporated into the latter. So, the presence of metallic nickel (Ni^0) on the surface of the catalyst seems be an important factor in determining its activity.

Binding energies for Ni^0 of ca. 850eV, which were observed in the spectra of the highly active catalysts, are, most likely, due to differentially charging. This usually happens with large particles and with particles having no good electrical contact with the support. A possibility could be that these Ni particles have been detached from the support by the carbon (sitting on carbon filaments). The Ni particles could thus be embedded in carbon matter of good electrical conductivity, which would render them in a different charging than the support and the Ni particles on it.

For all catalysts with Ni^0 on their surface, a carbon signal with low BE was observed. According to its binding energy this peak could be due to carbide species [17], which might suggest the involvement of nickel carbide species in the reaction. On the other hand, as all these samples contain differentially charged Ni^0 (see Fig. 1), the low-BE state might be also due to carbon with the same charging state as the differentially charged Ni^0, i.e., filamentous carbon.

5. Conclusions

(1) The application of calcium aluminate mixed oxides with varying bulk phase CaO to Al_2O_3 molar ratios and calcination temperatures, as support material for nickel leads to the production of totally different catalysts, concerning their surface properties, as well as, their catalytic performance.

(2) Metallic nickel was proven to be the active species for the methane partial oxidation reaction. The presence of differentially charged metal was also suggested from the XPS analysis of nickel spectra for the used catalysts. These are, most likely, Ni^0 particles that have been detached from the support and embedded in carbon matter of good electrical conductivity.

(3) The low carbon peak that was observed for all catalysts with Ni^0 on their surface could be due to carbide species or to carbon with the same charging state as the differentially charged Ni^0, i.e., filamentous carbon.

(4) A drastic decrease on the nickel dispersion for the catalysts with high nickel content was observed during the reaction. This could be attributed either to agglomeration or preferential depositing of carbon species on the nickel metal particles. Carbon deposition was also observed on the surface of the 5 wt% nickel catalysts after prolonged reaction.

(5) The activity and the selectivity of the high nickel content catalyst supported on the calcium aluminate with the lower CaO to Al_2O_3 molar ratio was unchanged after 20h of time on stream, even though carbon has been on its surface.

(6) No remarkable changes on the dispersion and on the nickel to carbon surface ratio were observed for the low nickel (1 wt%) content catalysts. Their difference in the catalytic activity for the methane partial oxidation reaction was ascribed to varying degree of reducibility of their surface nickel species.

Acknowledgements

The authors gratefully acknowledge the financial support of the EEC (JOU2-CT92-0073 and CHRX-CT93-0280 projects). Thanks are also due to A. Stambouli for catalyst testing.

References

[1] D. Dissanayake, M.P. Rosynek, K.C.C. Kharas and J.H. Lunsford, J. Catal., 132 (1991) 117.

[2] V.R. Choudhary and A.M. Rajput, J. Catal., 139 (1993) 326.

[3] S.M. Jackson, S.J. Thomsoin and G. Webb, J. Catal., 70 (1981) 249.

[4] W.J.M. Vermeiren, E. Blomsma and P.A. Jacobs, Catal. Today, 13 (1992) 427.

[5] D.A. Goetsch and G.R. Say, US patent 4, 877, 550 (1989).

[6] D.A. Goetsch, G.R. Say, J.M. Vargas and P.E. Ebexly, US patent 4, 888, 131 (1989).

[7] A.A. Lemonidou and I.A. Vasalos, Appl. Catal., 54 (1989) 119.

[8] T. Tomita, Proc. Pan-Pacific Synfuels Conf., Tokyo, 1982, p. 31.

[9] A.A. Lemonidou, PhD Thesis, Aristotelian University of Thessaloniki, 1990.

[10] J.H. Scofield, J. Electron. Spectrosc. Relat. Phenom., 8 (1976) 129.

[11] K.T. Ng and D.M. Hercules, J. Phys. Chem., 80(19) (1976) 2094.

[12] R.B. Shalvoy, P.J. Reucroft and B.H. Davis, J. Catal., 56 (1979) 336.

[13] F. Medina, P. Salagre, J.E. Sueiras and J.L.G. Fierro, J. Chem. Soc. Faraday Trans., 89(18) (1993) 3507.

[14] D. Dissanayake, M.P. Rosynek, K.C.C. Kharas and J.H. Lunsford, J. Catal., 132 (1991) 117.

[15] S.C. Tsang, J.B. Claridgfe and M.L.H. Green, Catalysis Today, 23 (1995) 3.

[16] M.A. Goula, A.A. Lemonidou and A.M. Efstathiou, J. Catal, in press.

[17] C.H. Bartholomew, Catal. Rev.-Sci. Eng., 24(1) (1982) 67–112.